Results

Part A: Photosystem I with artificial quinones

As described in the introduction (Chapter 2), the functional significance of many structural features of the quinone binding in PS I remains unclear. This is particularly evident when the cofactors and their binding sites are compared in the two types of RC's. Within this basic structure, the properties of all components show a great deal of variability. Sometimes the same quinone has been shown to function in either type of RC. The X-ray structure of PS I has confirmed the difference in orientation of phylloquinone (PhQ) in the type I RC of Photosystem I *versus* ubiquinone in the type II RC of purple bacteria (pbRC) [1, 4]. Both quinones have a methyl group and an unsaturated hydrophobic tail as ring substituents in adjacent positions between the two C=O groups. However, the interactions between quinone and protein, such as hydrogen bonding and π-stacking, are different (Figure 6.1). For instance, it is known that the redox potentials, H-bonding, electron transfer kinetics and magnetic tensor properties of the quinones in the two RCs differ greatly but it is not yet clear whether there is a correlated interplay between these various properties.

In the Part A of the thesis results from the PS I complexes with artificial quinones will be discussed. The artificial quinones were chosen to check the significance of certain structural elements such as methyl, ethyl and phytyl substituents on the quinone binding in PS I. Selective isotope labels ^{2}H and ^{13}C were introduced into chosen positions of the artificial quinones to gain more information about the spin density distribution and its asymmetry.

For the sample preparation, two different methods were applied: reconstitution of the quinone into the PS I complex after extraction of the native PhQ with organic solvent

or *in vitro* quinone exchange in the PS I complexes isolated from *menB* biosynthetic pathway mutant. According to the TR-EPR check of the radical pair state $P_{700}^{+}Q^{-}$ both methods gave comparable results. Thus the quinone and P_{700} environments were unaffected and the orientation and magnetic resonance properties of the cofactors remain identical for the two different kinds of preparations.

6. Orientation and protein-cofactor interactions of monosubstituted n-alkyl naphthoquinones in the A_1 binding site of Photosystem I

In this part, the results obtained for a series of naphthoquinone (NQ) derivatives with a single asymmetric ring substituent of n-alkyl character [-$(CH_2)_{(n-1)}$-CH_3] (there n is from n=0 to n=6) incorporated into PS I particles are presented. The primary goal was to determine the structural and functional specific role of the phytyl tail and of the -CH_3 group respectively in determining the orientation of the quinone headgroup and its binding to the protein. Hydrogen bonding and π-stacking interactions are known to be essential for the quinone binding [2]. However, it is not known how the methyl and phytyl substituents influence these features individually. One series, 1,4-naphthoquinone, 2-methyl-1,4-naphthoquinone (Vitamin K_3), 2-phytyl-3-methyl-1,4-naphthoquinone (PhQ) is useful to test the necessity of both methyl group and phytyl tail or only the methyl group for fixing the proper orientation and function of the quinone in the A_1 site. Another series of quinones with a single saturated alkyl chain of variable length (Figure 6.1b) is intended to replace the native phytyl tail with an alternative simpler chain.

6.1 General strategy

The molecular structures of the series of 1,4-naphthoquinone (NQ) derivatives introduced into the A_1 site of PS I are shown in Figure 6.2. Selective deuteration of methylene protons Figure 6.2b as well as total deuteration of the quinone molecules Figure 6.2c helps to get additional information from the TR-EPR spectra as will be explained late.

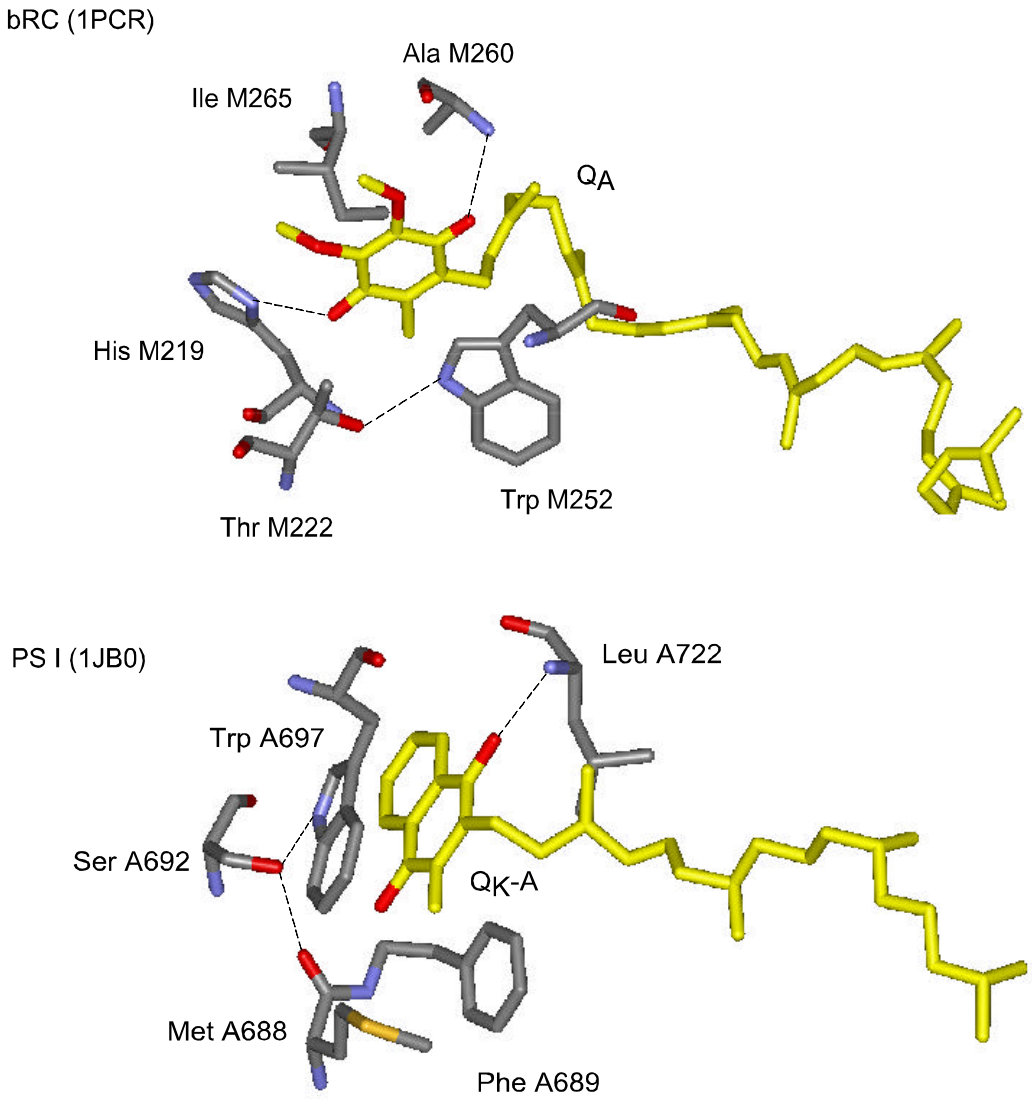

Figure 6.1 Top: Binding pocket of Q_A in the M subunit of reaction centers from *Rhodobacter sphaeroides*. Hydrogen bonds between the quinone carbonyl oxygens and M260 (peptide NH) and M219 (His-N_δH) are shown as dotted lines (PDB entry 1PCR, *Rb. Sphaeroides*).

Bottom: Structural model of the Q_K-A binding site in PS I as adapted from [1], (PDB entry 1JB0, *S. elongatus*). Residues are shown explicitly for those amino acids that are involved in identified protein-quinone interactions (p-stacking and H-bonding). The residues Trp (p- stacking) and Ser (part of H-bond network near Q_K-A).

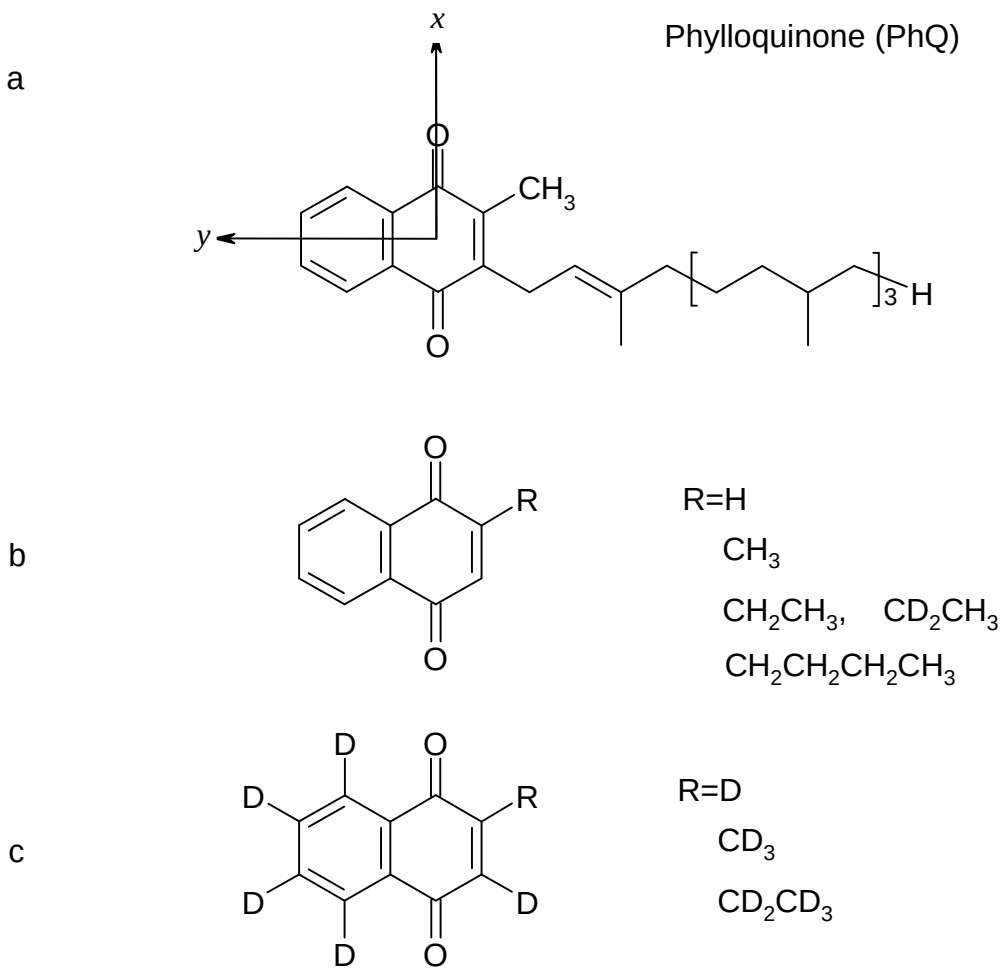

Figure 6.2 Molecular structure of naphthoquinone derivatives used.

a) Molecular structure of phylloquinone (PhQ (vitamin K_1), 2-methyl-3-phytyl-1,4-naphthoquinone) and g-tensor principal axes coinciding with the long and short inplane axes of the quinone ring. Note that the principal axes of the hfs tensors of the protons in the substituents deviate from the molecular x, y and z axes, *e.g.* $A_{\|}$ for the nearly axially symmetric CH_3 hfs tensor is roughly parallel to the C-CH_3 bond.

b) Molecular structures of the protonated and partially deuterated 1,4-naphthoquinone derivatives used for incorporation into the A_1 site in PS I.

c) Molecular structures of the corresponding fully deuterated 1,4-naphthoquinone derivatives.

For example, if the tail is not critical for quinone binding, with 2-methyl-1,4-naphthoquinone (VK_3) (*i.e.* n=1), it is expected that the quinone will be incorporated with the methyl group in the same position as the methyl group in PhQ, *i. e.* meta to the H-bonded oxygen. On the other hand, for larger values of n, it is expected for simple space filling reasons that the alkyl group will assume the role of the phytyl tail in PhQ and the quinone will bind with the alkyl group ortho to the H-bonded oxygen. The hyperfine couplings of the alkyl substituents serve as an ideal observable for determining the location of the substituents relative to the H-bonded oxygen because they are conveniently measured and reflect the asymmetry in the spin density distribution induced by the asymmetric H-bonding. The correct assignment of the hyperfine coupling to methyl and/or methylene protons can be assured unambiguously by selective deuteration. Finally, full deuteration of the 1,4-naphthoquinone derivatives (Figure 6.2c) is employed in order to reduce the hyperfine splittings and therefore the inhomogeneous linewidth. This effectively increases the *g*-tensor resolution and hence the accuracy in determining the orientation. Transient spin polarized EPR spectra of the functional radical pair state $P_{700}^{+}Q^{-}$ contain information about the relative orientation of the cofactors involved, as well as about specific interactions with the protein environment via the hyperfine and g-tensor parameters [33, 66]. Thus, they provide a convenient way of investigating the influence of NQ substituents on these binding properties.

6.2 Test of functionality of PS I particles after A_1 extraction / substitution.

By definition, the procedure used to remove PhQ denatures the A_1 binding site and leads to extraction of chlorophylls and catotenoids cofactors. Therefore, it is important to ensure that this process is reversible by cofactor reconstitution and that no permanent

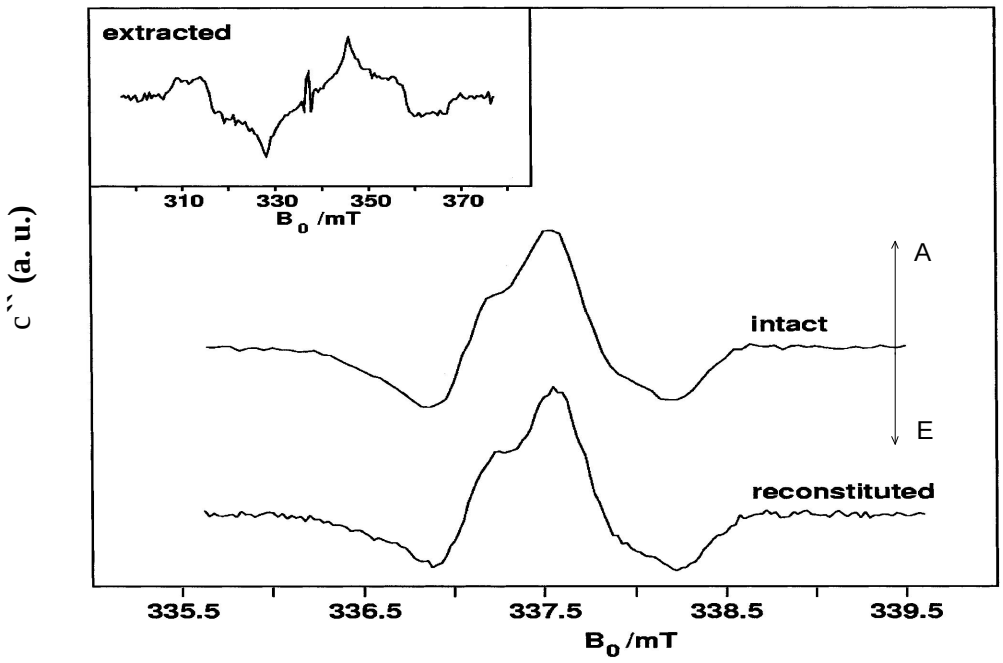

Figure 6.3 Spin polarized transient EPR spectra of $P_{700}^{+}A_1^{-}$ in PS I taken at X-band and 135 K before extraction (intact) and after extraction (extracted) and after reconstitution with PhQ (reconstituted). The inset shows the broad $^3P_{700}$ triplet spectra observed after extraction of the quinone. The small peaks at the center of the triplet spectrum are due to the small remaining fraction of reaction centers in which PhQ has not been removed. Note that the field axis covers a much wider range in the inset than in the main part of the figure.

damage or protein conformation changes occur. Figure 6.3 shows the result of a control experiment in which the extracted PS I has been reconstituted with PhQ. In the main part of Figure 6.3, the extracted PS I spin polarized transient EPR spectra of $P_{700}^{+}A_1^{-}$ are compared for intact PS I (top) and reconstituted with PhQ (bottom). The spectrum of PS I with extracted PhQ before reconstitution is shown on a expanded field scale as an inset. The broad spectrum in the inset is due to the characteristic polarization pattern of $^3P_{700}$ state and it corresponds to the PS I reaction centers devoid of PhQ [13]. The weak narrow peaks at the center of the inset spectrum are due to a minor fraction of reaction centers in which PhQ has not been removed. Clearly, incubation with PhQ (bottom spectrum)

restores electron transfer to the quinone as indicated in the resulting $P_{700}^{+}A_1^{-}$ spectrum. The electron transfer kinetics (not shown) are identical to those of intact PS I. Thus, we can conclude that the solvent extraction does not cause observable changes to the A_1-site and hence to the protein in the vicinity of the electron transfer chain from P_{700} to A_1. On the other hand, the organic solvent treatment is known to remove a considerable fraction of the antenna chlorophylls and carotenoids. We cannot exclude that a portion of the reaction centers becomes inactive as a result of the quinone extraction/reconstitution procedure. An estimate from a comparison of the signal-to-noise ratios in Figure 6.3 is inappropriate because identical instrumental conditions cannot be guaranteed in this case.

An additional check is possible if the incorporation of artificial quinone is done by the *in vitro* substitution of plastoquinone-9 in the PS I particles from *menB* mutant. The former method has a distinct advantage over the organic solvent extraction method in that PS I complexes remain unaffected during the quinone exchange. The carotenoids and chlorophylls are preserved as in the native state. In general, *in vitro* quinone replacement in PS I complexes from the *menB* mutant will leave the PSI complexes intact. In practice, a higher signal to noise ratio is achieved in the TR EPR spectra of functional radical pair $P_{700}^{+}NQ^{-}$ using the *in vitro* displacement method.

The experiments with the organic solvent quinone extraction/reconstitution in the wild type PS I and PQ-9 exchange in the PS I from *menB* mutant were performed in parallel with the same quinone series. The results of TR EPR study of samples prepared by two different methods are identical, thus, data obtained for samples prepared by only one method will be presented.

6.3 PS I containing 2- alkyl NQ derivatives

Figure 6.4 presents the X-band and Q-band spectra of the radical pair state $P_{700}^{+}Q^{-}$ in a series of PS I samples containing 2-methyl-, 2-ethyl- and 2-butyl-1,4-naphthoquinone. The transient EPR spectra of the three samples exhibit the same overall polarization pattern as native PS I, *i.e.* E/A/E (E=emission, A=absorption) at X-band and E/A/A/E/A at Q-band (Figure 6.4). While the overall polarization pattern does not change, the non-native quinones do have a dramatic effect on the partially resolved proton hyperfine structure (hfs). For native PS I, the methyl group in the meta position to the H-bonded oxygen (Figure 6.1) leads to a resolved quartet with relative intensities 1:3:3:1 centered near the g_{yy}-component of the quinone g-tensor as result of a nearly axially symmetric hfs tensor. Principal values of this tensor were determined with high precision by ENDOR spectroscopy of the A_1^{-} photoaccumulated radical (A_{xx} = 9.1 MHz, A_{yy} = 12.8 MHz, A_{zz} = 9.1 MHz) [40] and for the charged separated state $P_{700}^{+}A_1^{-}$ (A_{xx} = 8.8 MHz, A_{yy} = 12.3 MHz, A_{zz} = 8.8 MHz) [67]. The same hfs pattern is even more clearly resolved in the spectra from the samples incubated with 2-methyl-1,4-NQ (VK_3) (Figure 6.4, second spectrum from top). This is readily explained if the spin density distribution over the NQ rings remains the same as for PhQ but the inhomogeneous linewidth is reduced due the smaller number of unresolved proton hyperfine couplings when the nearby phytyl tail is absent. In native PS I, the partially resolved methyl hyperfine splitting is unusually large because the oxygen meta to the methyl group is involved in H-bonding while the oxygen ortho to it is not [1, 68]. This results in an alternating spin density distribution such that the spin density is increased on the ring carbon to which the methyl group is bound [66, 68, 69]. Thus, the spin polarization and hyperfine pattern observed with 2-methyl-1,4-NQ in the A_1 binding site suggest that it binds to the protein with the methyl group in the same position as for native PhQ.

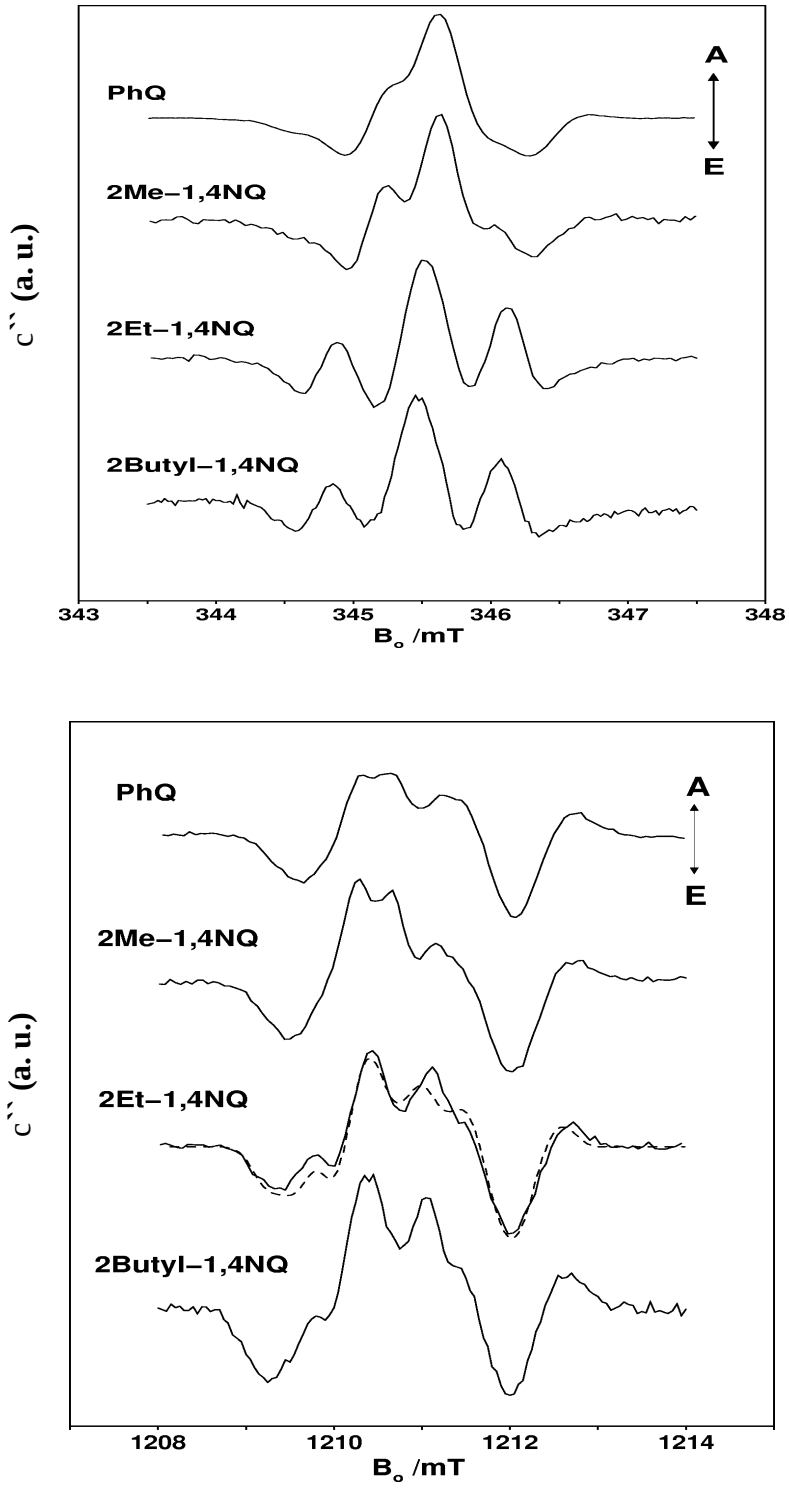

Figure 6.4 Top: X-band, 80K spin polarized transient EPR spectra of $P_{700}^{+}Q^{-}$ radical pair in PS I containing native phylloquinone (PhQ), 2-methyl, 2-ethyl and 2-butyl-1,4-naphthoquinone in the A_1 binding site. Bottom: corresponding Q-band, 80K spin polarized transient EPR spectra of the same samples. The broken line curve is a simulated spectrum, calculated using the parameters given in Table 6.1.

In contrast, the well resolved hfs-triplet with relative intensities 1:2:1 observed for the samples incubated with 2-ethyl- and 2-butyl-1,4-NQ (bottom spectra in Figure 6.4) has no correspondence in native PS I. The splitting pattern is due to two nearly equivalent protons and is assigned to the first methylene group of the alkyl chain.

In order to verify this assignment independently, selective deuteration of the methylene group of 2-ethyl-1,4-NQ was used. As demonstrated in Figure 6.5, the 1:2:1 hyperfine pattern disappears if the methylene group of 2-ethyl-1,4-NQ is selectively deuterated (bottom spectrum in Figure 6.5). The splitting of the partially resolved hyperfine pattern gives an effective hfs constant for the methylene protons. A rough estimate from a qualitative inspection of spectra in Figure 6.5 yields a value of 16-17 MHz which is considerably larger than that of the methyl protons of 2-methyl-1,4-NQ.

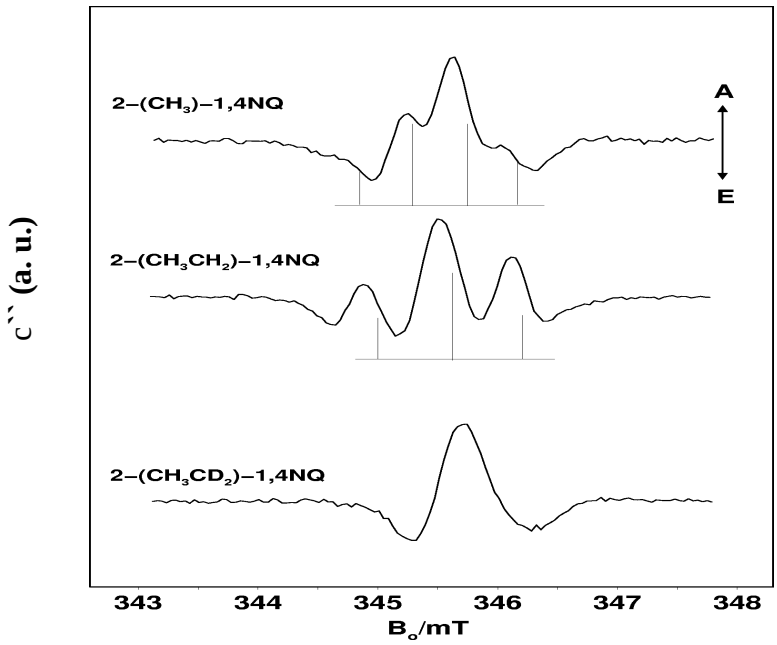

Figure 6.5 X-band, 80K spin polarized transient EPR spectra of $P_{700}^{+}NQ^{-}$ in PS I with 2-methyl, 2-ethyl and 2-ethyl-α,α-d_2-1,4-naphthoquinone in the A_1 binding site. The characteristic hfs 1:3:3:1 for $–CH_3$ group and 1:2.1 for $–CH_2$- group are indicated.

Thus, the spin density on the ring carbon adjacent to the alkyl group must be high. Consequently, the distortion of the spin density due to asymmetric H-bonding is such that the alkyl group has to be meta to the oxygen with the H-bond. If the 2-alkyl-1,4-NQ's are also bound to the protein via a single H-bond to Leu A722 (B706), this places the alkyl side chains in a position analogous to the methyl group in phylloquinone. This is a surprising result because one would expect that with increasing chain length, steric hindrance would force the alkyl chain to reside in the space normally occupied by the phytyl tail of PhQ. Indeed, we have recently shown [44] that this occurs when 2-phytyl-1,4-NQ is incorporated into PS I by inhibiting the final methylation step in the biosynthesis of PhQ. In this case, a strong hfs is observed from the ring proton in the position occupied by the methyl group in PhQ, while the hfs from the methylene protons of the phytyl tail is too small to be resolved (for summary see Table 7.1). Thus, as for PhQ, the ring carbon to which the phytyl tail is attached carries a low spin density because it is ortho to the H-bonded oxygen while the methyl group in PhQ and the ring proton in 2-phytyl-1,4-NQ of the *men*G mutant are meta to the H-bonded oxygen. In contrast, for ethyl- and butyl-1,4-NQ and longer n-alkyl-1,4-NQ (not shown) the situation is obviously reversed with the alkyl tail now meta to the H-bonded oxygen and the ring proton in the ortho position.

6.4 Orientation of alkyl NQ's in A_1 site

The unexpected tail position could be related to a different orientation of the quinone headgroup in the protein. The spin polarization pattern of the $P_{700}^{+}Q^{-}$ state is known to be particularly sensitive to the relative orientation of the g-tensors $\mathbf{g}(P_{700}^{+})$ and $\mathbf{g}(NQ^{-})$ with respect to the vector $\mathbf{z}_D$ connecting the spin density centers of the respective

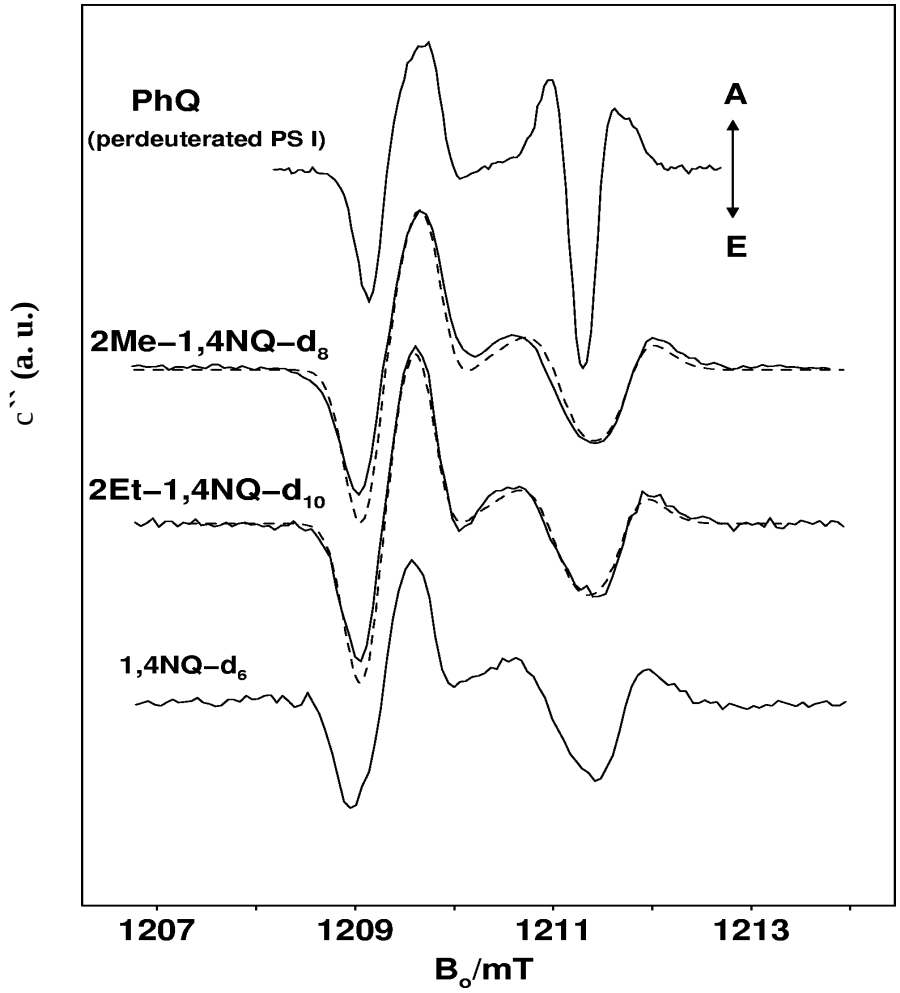

Figure 6.6 Q-band, 80K spin polarized transient EPR spectra of $P_{700}^{+}Q^{-}$ in PS I. Comparison from top to bottom of deuterated PS I, deuterated and 2-methyl, 2-ethyl-1,4-naphthoquinones and deuterated 1,4-naphthoquinone in the A_1 binding site. Broken lines are simulated spectra, for simulation parameters see in Table 6.1.

radical ions [33]. To evaluate the relative orientation of the g-tensors, the spectral components corresponding to the principal g-values must be well-resolved, i. e. high field/frequency EPR spectra are required. For samples containing deuterated quinones, the

Q-band (35 GHz) spectra shown in Figure 6.6 are sufficiently well-resolved to allow the quinone orientation to be determined. The features on the low-field side of the spectra are known to be due to only the quinone, while the spectral contributions on the high-field side are mainly determined by P_{700}^{+}. Correspondingly, the up-field A/E/A feature is narrowed only in the top spectrum of Figure 6.6, when the chlorophylls of P_{700} are also deuterated along with the rest of the reaction center. For the other spectra only the NQ cofactor is fully deuterated. Figure 6.6 includes simulations (broken lines) of the spectra of PS I containing perdeuterated 2-ethyl- and 2-methyl-1,4-NQ using the same orientation of the quinone ring plane as known for phylloquinone in native PS I. The simulation parameters are collected in Table 6.1.

Table 6.1: g-tensor and geometrical parameters obtained from simulations of the transient EPR spectra of $P_{700}^{+}NQ^{-}$

	g_{xx}	g_{yy}	g_{zz}	$\Delta B(Q^{-})$ mT	α_p	β_p	γ_p	θ_D	φ_D
PhQ-d_{46}	2.0062	2.0051	2.0022	0.25	81.0	126.0	182.0	90.0	0
2- Methyl-1,4-NQ	2.0063	2.0051	2.0024	0.34	81.0	126.0	182.0	90.0	0
2- Ethyl -1,4-NQ	2.0063	2.0052	2.0022	0.31	81.0	126.0	182.0	90.0	0
2-Ethyl-α,α-d_2-1,4NQ	2.0063	2.0052	2.0022	0.36	81.0	126.0	182.0	90.0	0
2-Ethyl-1,4-NQ-d_{10}	2.0063	2.0052	2.0022	0.34	81.0	126.0	182.0	90.0	0

PhQ-d_{46} – perdeuterated phylloquinone in perdeuterated PS I complexes [66].

ΔB – peak to peak linewidth in first derivative spectra. $\Delta B(P_{700}^{+}) = 0.31$mT

The Euler angles α_p, β_p, γ_p describe the relative orientation of $\mathbf{g}(P_{700}^{\cdot+})$ and $\mathbf{g}(Q^{\cdot-})$ [66]

The polar and azimuthal angels θ_D and φ_D describe the orientation of $\mathbf{z}_D$ relative to $\mathbf{g}(Q^{\cdot-})$

Dipolar and isotropic spin-spin couplings: D=-170 μT, J=1 μT.

Note, that slight differences in the g-tensor values between the WT and artificial quinones were obtained during the simulation procedure, independent precise determination of those parameters is possible at W-band. The fact that the experimental patterns can be simulated with the same orientation parameters suggests that both non-native quinones bind with the same headgroup orientation. Moreover, it was shown previously that the distance between P_{700}^{+} and Q^{-} is the same as that in native PS I for a variety of non-native quinones [70].

With the PQ vector oriented along the *x*-axis of the quinone g-tensor, (see Table 6.1) four orientations for the quinone headgroup are possible. The relative orientation of the hfs tensor as well as the hyperfine couplings, which show that the alkyl tail is meta to the H-bonded oxygen, allow the number of possible orientations to be reduced to two. One of the remaining orientations places the side chains of the 2-alkyl-1,4-NQ where the second aromatic ring of phylloquinone is usually located. Such an arrangement is very unlikely because it would lead to steric crowding and would weaken the π–π interaction between the quinone and the neighbouring tryptophan. Therefore, we conclude from the EPR data that the alkyl chains are attached to the ring position normally occupied by the methyl group.

The bottom spectrum in Figure 6.6 shows 1,4-NQ-d_6 reconstituted into PS I. The E/A/A/E/A polarization pattern with slightly broadened low field features is significantly different from that reported previously [71]. In the earlier study the polarization pattern for 1,4-NQ-d_6 was A/E/A/A/E/E compared to E/A/A/E/A for PhQ in PS I. The change in the polarization pattern was best explained by a change in orientation from $\mathbf{z}_D$ || x (PhQ) to nearly $\mathbf{z}_D$ || y (1,4-NQ), while the orientation of the z-axis remained unchanged. The different polarization patterns measured for different preparations show that the orientation

of NQ in PS I may depend on details of the sample preparation procedure. A systematic study of the extraction conditions revealed that successful extraction of the quinone depends crucially on the purity of the hexane used. Since the orientation reported in [71] ($\mathbf{z}_D$ || y (1,4-NQ)), is incompatible with an H-bond to Leu A722 (B706) it is likely that the loop region containing the leucine may be affected by the presence or absence of an impurity in the hexane. The broadened spectrum for 1,4-NQ in Figure 6.6 is consistent with a distribution of orientations of the substituted 1,4-NQ molecule perhaps due to a distribution of somewhat different binding site conformations. Such a distribution may also be a consequence of the fact that the 1,4-NQ molecule is the smallest and the only one studied here that does not have an asymmetric substituent. The degree of hydrogen bonding of 1,4-NQ is also reflected in its g-tensor. The principal values of the g-tensor of A_1^- are known to depend on the presence and strength of H-bonds [66] and in general, the *g*-tensor anisotropy of semiquinone and related radicals decreases with formation of hydrogen bonds [72, 73, 74]. π-stacking interaction is known to have an opposite influence on the *g*-tensor and increases its anisotropy. In keeping with the altered orientation, which necessarily breaks the H-bond to Leu A722 (B706), the g-tensor anisotropy for 1,4-NQ-d_6 incorporated into PS I reported in [46] is larger than that of the native PhQ [75, 76]. However, from Figure 6.6 it is apparent that when 1,4-NQ-d_6 is oriented in the same way as PhQ in the A_1 site, its g-tensor anisotropy is also very similar suggesting that the H-bond Leu A722 (B706) is intact.

6.5 Evaluation of hyperfine coupling

The well-resolved 1:2:1 hyperfine pattern (see Figures 6.4 and 6.5) indicates strong hyperfine coupling to the methylene protons.

The value of the isotropic coupling constant of such β-protons (e.g. of an ethyl or butyl substituent) is known to be proportional to the π-spin density at the neighbouring ring carbon atom ($\rho_c^{(\pi)}$) and to $\cos^2\theta$:

$$a_{iso}(H_\beta)=\rho_c^{(\pi)}(B_0+B_2\cos^2\theta), \quad (1)$$

where θ is the dihedral angle between the plane of the C-C and C-H bonds and the axis of the p_z orbital (see Figure 6.7). Standard values for the constants are B_0 = 9 MHz and B_2 = 122 MHz [77]. The experimental hyperfine patterns in Figures 6.4 and 6.5 show that the two hydrogen atoms of the -CH_2- group are magnetically equivalent within experimental accuracy. To that extent, the dihedral angle θ must be the same for both hydrogens as well. Only two conformations of the C – CH_2 – C fragment fulfil this requirement. Either the two C – C bonds are in-plane with respect to the NQ ring and both C-H bonds have θ = 30° as shown in Figure 6.7 or the second C – C bond points maximally out-of-plane and both C-H bonds have θ = 60°. The $\cos^2\theta$ factor leads to a methylene proton hfs, which is three times larger in the former case. To calculate the hyperfine couplings for these two possibilities, we need the value of the spin density $\rho_c^{(\pi)}$ on the neighbouring ring carbon. This values can be obtained by two independent methods either using a_{iso}=10.0 MHz of the methyl group and equation $a_{iso}(CH_3)=\rho_c^{(\pi)}(B_0+B_2\cos^2\theta)$ with the θ=45° (this angle corresponds to average possible dihedral angle because of the fast rotation of the methyl group) or using a_{iso}= -10.3 MHz of the α-proton recalculated from the hfs-tensor measured by ENDOR spectroscopy for 2-phytyl-1,4-naphthoquinone in the A_1 site of PS I from *menG* mutant [44] and the equation $a_{iso}(CH)=\rho_c^{(\pi)}Q_{CH}$, Q_{CH}=-64,8 MHz. $\rho_c^{(\pi)}$=0.14 and $\rho_c^{(\pi)}$=0.16 are results for the first and second methods respectively. They can be averaged to $\rho_c^{(\pi)}$=0.15. With this spin density, only the configuration of the methylene protons with cosθ=30° can be reconciled with the data. We

obtain $|A_{xx}|$ = 12.2 MHz, $|A_{yy}|$ = 16.8 MHz, $|A_{zz}|$ = 12.2 MHz and a_{iso} = 13.7 MHz from simulation of the 2-ethyl-1,4-NQ spectrum shown in Figure 6.4 (bottom). This corresponds to θ = 34° and is indistinguishable from θ = 30° within experimental accuracy. The θ = 60° conformation cannot be completely excluded but it would require a spin density on the carbon which is three times higher than the already large value found in native PS I. It is very unlikely that such a high spin density would occur. In summary the most likely configuration is that the alkyl tail resides in the position normally occupied by the methyl group and is oriented so that the two protons straddle the ring plane. A potentially interesting aspect is revealed by the simulation results of Table 6.1. The inhomogeneous linewidth contribution for A_1 in fully deuterated PS I is substantially smaller than that needed for deuterated NQ derivatives in otherwise protonated PS I despite the fact that the two substituents of PhQ should lead to a somewhat larger linewidth than for the monosubstituted NQ derivatives.

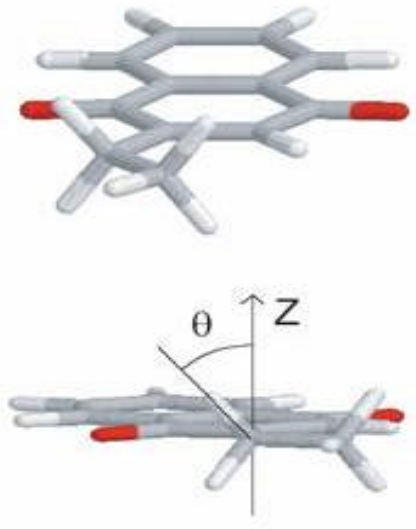

Figure 6.7 Conformation of the ethyl substituent in the 2-ethyl-1,4-naphthoquinone molecule in the A_1 site PS I as obtained from the analysis of the hyperfine structure. z denotes the out-of-plane axis and is equivalent to the p_z orbital axis of the carbon ring atom. θ = 30° is the dihedral angel between the plane of the C-C and C-H bonds in ethyl group and the axis of the p_z orbital.

This may be indicative of a substantial hyperfine coupling to the proton in the H-bond because this coupling will be reduced in fully deuterated PS I but remains the same when only the quinone is deuterated. For this reason the samples with fully deuterated quinones with normal hydrogen in the H-bond are best candidates for a reliable determination of hfs coupling to the H-bonding proton using the full arsenal of advanced pulsed EPR techniques. In particular pulsed ENDOR spectroscopy of the radical pair $P_{700}^{+}Q^{-}$ allows the quinone to be observed in the functional radical pair state rather than as a photoaccumulated radical.

6.6 Influence of asymmetric substitution on quinone binding in PS I

As it was demonstrated in this chapter, even a single methyl group, *i.e.* 2-methyl-1,4-NQ (VK_3) assures the same orientation of the NQ headgroup as that of native phylloquinone. An unexpected result was that the NQ's with a saturated alkyl chain as a single substituent bind in the A_1 site such that the alkyl chain assumes the position normally occupied by the phylloquinone methyl group and not that of phytyl chain. This implies that just one asymmetric substituent is sufficient for proper orientation and thus even a single methyl substituent does in fact play an essential role in determining the orientation of the headgroup in the A_1 site.

Our studies with substitution of 2-methyl-1,4-naphthoquinone in PS I of the *men*B mutant and a previous study of 2-phytyl-1,4-naphthoquinone after inhibition of the methyltransferase gene *men*G [44] have demonstrated that either the phytyl-tail or the methyl group can be left out but one of them (or any asymmetric (mono) substituent of 1,4-NQ) is necessary for maintaining the native quinone orientation and position in the A_1

site of PS I. In this study it has been found that the minimal structural component needed for maintaining 1,4-naphthoquinone in the correct orientation is a methyl group. 1,4-naphthoquinone without substituent or 1,4-naphthoquinone symmetrically substituted in the positions 2 and 3 (data not presented in the dissertation) orients differently or lead to a distribution of different orientations. In this chapter, the question was asked how an alternative chain (like a saturated n-alkyl chain in the simplest case) would behave. The transient EPR data for 2-methyl-1,4-naphthoquinone (VK_3) substituted into A_1-free PS I are shown here to be indistinguishable from those obtained with the same 2-methyl-1,4-naphthoquinone exchanged *in vitro* for the PQ-9 in the *men*B mutant [41]. In contrast, when 2-ethyl, 2-butyl (and even longer 2-alkyl)-1,4-naphthoquinones are substituted in PS I, the A_1 site places the artificial quinone with the substituent not in the position where the phytyl-tail of native PhQ is normally located but rather in the position usually occupied by the methyl group. Initial attempts to model the non-native quinones in the A_1 binding site suggest that with this configuration and with the methylene protons straddling the ring, the alkyl tail was also directed towards the space normally occupied by the phytyl tail of PhQ. However, there are no obvious reasons why this could not be achieved equally well with the alkyl-tail in the ring position normally occupied by the phytyl tail in native PhQ. The double bond in the phytyl tail may also play a significant role.

The methyl group in PhQ certainly adds a contribution to the binding strength of the naphthoquinone headgroup. However, it remains unclear why this extra binding strength would be needed since there does not appear to be any significant selective pressure from poor physiological performance when the methyl group is absent (example: 2-phytyl-1,4-NQ in *menG* mutant). Note also, that forward electron transfer from the A_1 site to the first FeS center is slowed down without the methyl group compared to wild type [44]. It is slowed down even further (beyond the limited detectability range of the TR-EPR

method) for all 2-alkyl-1,4-naphthoquinones investigated in this study. The preliminary hypothesis is that the charge distribution and charge control are important for the quinone function. The asymmetric hydrogen bond induces the asymmetry in charge distribution as shown in Figure 7.3. Asymmetric substitution can stabilize or destabilize a quinone charged state via the inductive effect.